Novel Donepezil-Based Inhibitors of Acetyl- and Butyrylcholinesterase and Acetylcholinesterase-Induced β-Amyloid Aggregation

Pelayo Camps,*[,†] Xavier Formosa,[†] Carles Galdeano,[†] Tània Gómez,[†] Diego Muñoz-Torrero,*[,†] Michele Scarpellini,[†] Elisabet Viayna,[†] Albert Badia,[‡] M. Victòria Clos,[‡] Antoni Camins,[§] Mercè Pallàs,[§] Manuela Bartolini,[#] Francesca Mancini,[#] Vincenza Andrisano,[#] Joan Estelrich,[||,⊥] Mònica Lizondo,[||,⊥] Axel Bidon-Chanal,[||] and F. Javier Luque[||]

Laboratori de Química Farmacèutica (Unitat Associada al CSIC), Facultat de Farmàcia, and Institut de Biomedicina (IBUB), Universitat de Barcelona, Av. Diagonal 643, E-08028, Barcelona, Spain, Departament de Farmacologia, de Terapèutica i de Toxicologia, Facultat de Medicina, Universitat Autònoma de Barcelona, E-08193-Bellaterra, Barcelona, Spain, Unitat de Farmacologia i Farmacognòsia, Facultat de Farmàcia, Universitat de Barcelona, Av. Diagonal 643, E-08028, Barcelona, Spain, Department of Pharmaceutical Sciences, Alma Mater Studiorum, Bologna University, Via Belmeloro 6, I-40126 Bologna, Italy, Departament de Fisicoquímica, Facultat de Farmàcia, and Institut de Biomedicina (IBUB), Universitat de Barcelona, Av. Diagonal 643, E-08028, Barcelona, Spain, and Institut de Nanociència i Nanotecnologia, Universitat de Barcelona, Barcelona, Spain

Received February 7, 2008

A novel series of donepezil−tacrine hybrids designed to simultaneously interact with the active, peripheral and midgorge binding sites of acetylcholinesterase (AChE) have been synthesized and tested for their ability to inhibit AChE, butyrylcholinesterase (BChE), and AChE-induced Aβ aggregation. These compounds consist of a unit of tacrine or 6-chlorotacrine, which occupies the same position as tacrine at the AChE active site, and the 5,6-dimethoxy-2-[(4-piperidinyl)methyl]-1-indanone moiety of donepezil (or the indane derivative thereof), whose position along the enzyme gorge and the peripheral site can be modulated by a suitable tether that connects tacrine and donepezil fragments. All of the new compounds are highly potent inhibitors of bovine and human AChE and BChE, exhibiting IC_{50} values in the subnanomolar or low nanomolar range in most cases. Moreover, six out of the eight hybrids of the series, particularly those bearing an indane moiety, exhibit a significant Aβ antiaggregating activity, which makes them promising anti-Alzheimer drug candidates.

Introduction

Since bis(7)-tacrine, a heptamethylene-linked dimer of the first marketed anti-Alzheimer drug tacrine (**1**, Chart 1), was developed 1 decade ago,[1–3] the search for inhibitors of acetylcholinesterase (AChE[a]) able to simultaneously bind to its catalytic and peripheral binding sites has become an area of very active research. Several classes of dual binding site AChE inhibitors have been developed by connecting through a suitable linker the two interacting units, which are generally derived from known AChE inhibitors either commercialized or under development.[2–8] The success of the dual binding site strategy is evidenced by the large increase in AChE inhibitory potency of these dimers or hybrids relative to the parent compounds from which they have been designed. Further interest comes from the fact that some of these dual binding site AChE inhibitors have been shown to inhibit the aggregation of β-amyloid peptide (Aβ),[9–18] which is a key event in the neurotoxic cascade of Alzheimer's disease (AD).[19] This effect, which has been related to the blockade of the AChE peripheral site[20] by dual binding site AChE inhibitors, makes these compounds very promising disease-modifying anti-Alzheimer drug candidates.

Chart 1. Structures of Tacrine, Donepezil, and the Known Donepezil−Tacrine Hybrids **3** and **4**

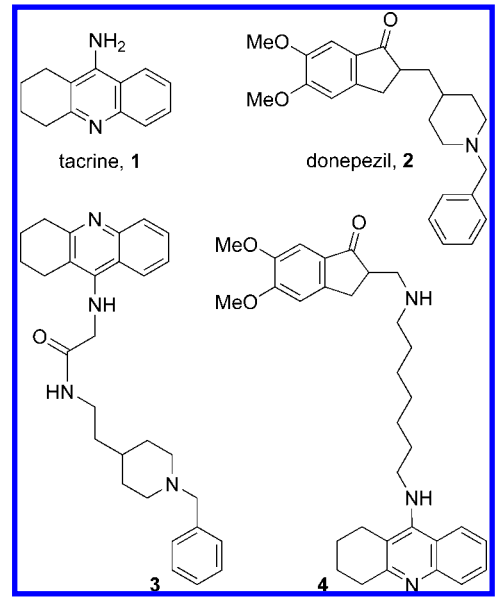

To date, the sole dual binding site AChE inhibitor approved for the treatment of AD is donepezil (**2**, Chart 1), though it was not specifically designed as such.[21] The X-ray crystallographic structure of the complex between *Torpedo californica* AChE (*Tc*AChE) and donepezil (PDB entry 1EVE)[22] shows that the

* To whom correspondence should be addressed. For P.C.: phone, +34 + 934024536; fax, + 34 + 934035941; e-mail, camps@ub.edu. For D.M.-T.: phone, +34 + 934024536; fax, + 34 + 934035941; e-mail, dmunoztorrero@ub.edu.

[†] Laboratori de Química Farmacèutica and IBUB, Universitat de Barcelona.

[‡] Universitat Autònoma de Barcelona.

[§] Unitat de Farmacologia i Farmacognòsia, Universitat de Barcelona.

[#] Bologna University.

[||] Departament de Fisicoquímica, Universitat de Barcelona.

[⊥] Institut de Nanociència i Nanotecnologia, Universitat de Barcelona.

[a] Abbreviations: Aβ, β-amyloid peptide; AChE, acetylcholinesterase; AChEI, acetylcholinesterase inhibitor; AD, Alzheimer's disease; APP, amyloid precursor protein; BChE, butyrylcholinesterase; DTNB, 5,5′-dithiobis(2-nitrobenzoic) acid; HFIP, 1,1,1,3,3,3-hexafluoro-2-propanol; MD, molecular dynamics; PDB, protein data bank; PTFE, polytetrafluoroethylene; rmsd, root-mean square deviation

10.1021/jm8001313 CCC: $40.75
Published on Web 06/03/2008

elongated structure of donepezil spans the entire length of the enzyme active-site gorge forming a variety of interactions with specific residues, such as aromatic stacking interactions between the benzyl and indanone moieties and the indole rings of Trp84 and Trp279 (Trp86 and Trp286 in human AChE) at the catalytic and peripheral sites, respectively, and the cation−π interaction between the protonated piperidine nitrogen and the phenyl ring of Phe330. As a result of its dual binding site character, donepezil at 100 μM is able to inhibit by 22% the AChE-induced aggregation of Aβ.[23] As bis(7)-tacrine, most of the dual binding site AChE inhibitors developed so far contain at least one unit related to tacrine, probably because of its ease of synthesis and its affinity for both the active and peripheral sites of AChE.[10–12,17,24–34] Conversely, to the best of our knowledge, only two classes of donepezil-based hybrids have been purposely designed as dual binding site AChE inhibitors by combining different fragments of donepezil with tacrine.[30,31] Among these donepezil−tacrine hybrids, compounds **3** and **4** (Chart 1), which retain the *N*-benzylpiperidine and the 5,6-dimethoxy-1-indanone moieties of donepezil, respectively, are the most potent, they being 37- and 7-fold more potent than tacrine but nearly equipotent to donepezil, while their Aβ-antiaggregating effect has not been assessed.

Herein, we describe the synthesis, pharmacological evaluation (AChE and butyrylcholinesterase (BChE) inhibition and Aβ-antiaggregating effect), and molecular modeling of a novel class of highly potent donepezil−tacrine hybrids. On the basis of the binding modes of donepezil[22] and tacrine[35] within *Tc*AChE, these novel hybrids were designed by combining the 5,6-dimethoxy-2-[(4-piperidinyl)methyl]-1-indanone moiety of donepezil with tacrine, which would thus replace the benzyl moiety of donepezil. In contrast to the preceding approaches,[30,31] the strategy adopted here largely preserves the chemical skeleton of donepezil, which should allow the new hybrid compounds not only to mimic the interactions of tacrine at the catalytic site and of the indanone ring at the peripheral one but also to preserve the contacts of the piperidine moiety with the residues that are lining the wall of the AChE gorge as a third binding site within the enzyme.

Chemistry

The structures of the novel donepezil−tacrine hybrids **14**−**15a**,**b** are shown in Scheme 1. The linker was selected taking into account the sizable increase in AChE inhibitory potency observed in tacrine-based homo- and heterodimers upon introduction in the tether of a protonatable amino group at a distance equivalent to three methylene groups.[28,29] Because this protonatable amino group could be the piperidine nitrogen atom of these donepezil−tacrine hybrids, a length of two to three methylenes for the linker was considered. Moreover, introduction of a chlorine atom at position 6 of the tacrine skeleton should lead to additional interactions within the active site of the enzyme.[36–38]

The synthesis of the novel donepezil−tacrine hybrids **14**−**15a**,**b** was carried out through a three-step sequence involving amination of the known 9-chloro-1,2,3,4-tetrahydroacridines **5** or **6**[39,40] with an ω-aminoalcohol **7**, followed by mesylation of the resulting alcohol **8** or **9** and subsequent reaction with the known piperidine **12**[21,41,42] (Scheme 1). Taking into account that both enantiomers of donepezil display similar pharmacologic and pharmacokinetic profiles and span the entire AChE gorge with a common pattern of interactions,[43] compounds **14**−**15a**,**b**, which bear the stereocenter-containing indanone unit of donepezil, were prepared in racemic form.

Scheme 1. Synthesis of the Donepezil−Tacrine Hybrids **14**−**17a**,**b**

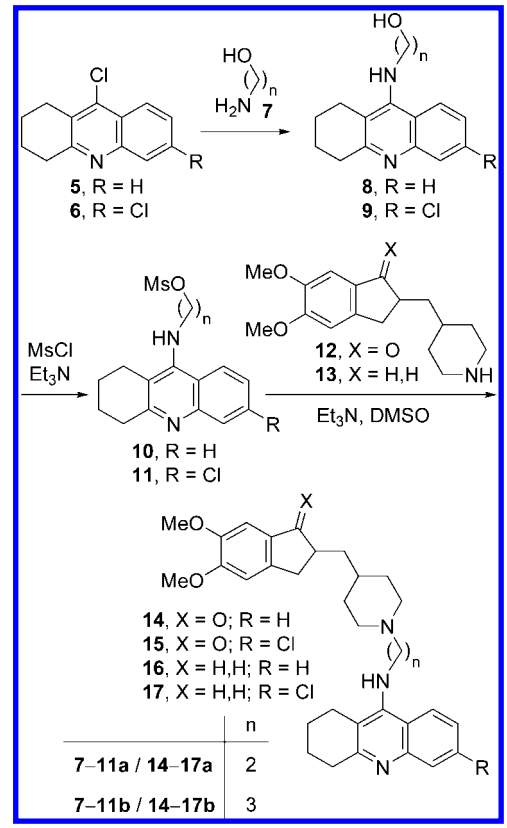

Moreover, because the indane derivative **13** is readily available,[44] the synthesis of a parallel series of achiral hybrids **16**−**17a**,**b** was also carried out by following the same methodology but using piperidine **13** in the last step instead of **12** (Scheme 1).

In a first approach, the amination of the chloroquinolines **5** and **6** was carried out on reaction with 3 equiv of 2-aminoethanol (**7a**) or 3-amino-1-propanol (**7b**) in refluxing 1-pentanol[45,46] for 18 h, followed by removal of the solvent and excess of aminoalcohol by distillation under reduced pressure. Alternatively, the change of this tedious microdistillation workup by a standard acid−base extraction turned out to be much more convenient for the isolation of the desired alcohols. In this way, the new alcohols **8a** and **9a**,**b** and the known alcohol **8b**[40] were obtained in excellent yields and used directly in the next reaction without further purification. However, for characterization purposes, the new alcohols **8a** and **9a**,**b** were transformed into their hydrochlorides and recrystallized from MeOH/AcOEt mixtures.

Mesylation of **8**-**9a**,**b** proceeded almost quantitatively, affording pure mesylates **10a**,**b** and **11a** and slightly impure **11b**, which were used directly in the following reaction.

Piperidine **12** was prepared in quantitative yield following a described procedure[42] based on the catalytic hydrogenation of donepezil in MeOH at 1 atm and room temperature for 72 h, while piperidine **13** was prepared in 82% yield by a new procedure involving the catalytic hydrogenation of donepezil hydrochloride in MeOH in the presence of 1 N HCl at 28 atm and 65 °C for 6 days (Scheme 2). Alternatively, **13** was prepared in better yield (92% overall) through a two-step procedure involving aldol condensation of 5,6-dimethoxy-1-indanone with pyridine-4-carboxaldehyde in the presence of *p*-TsOH·H_2O in refluxing toluene,[41] followed by catalytic hydrogenation of the resulting compound **18** under forcing conditions (Scheme 2).

Scheme 2. Synthesis of Piperidine **13** and the Indane Derivative of Donepezil **19**

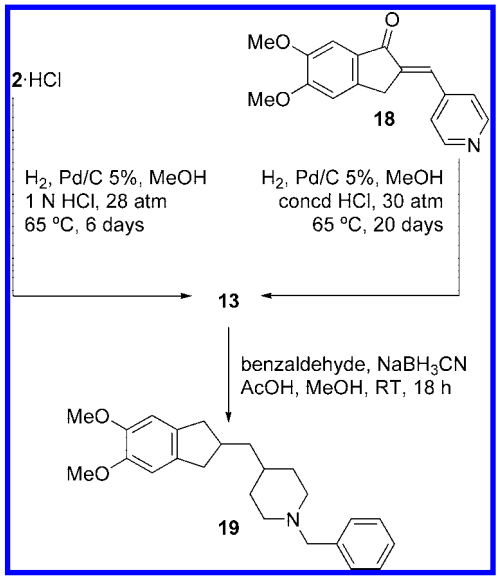

Finally, alkylation of piperidines **12** and **13** with a stoichiometric amount of mesylates **10**−**11a**,**b** in the presence of excess of Et_3N in DMSO at 85 °C for 2 days afforded the desired donepezil−tacrine hybrids **14**−**15a**,**b** and the indane derivatives **16**−**17a**,**b** in low to moderate yields (Scheme 1) after a tedious purification of the crude products by silica gel column chromatography.

For comparison purposes, the indane derivative of donepezil, **19** (Scheme 2), was also prepared. This compound can be prepared directly from donepezil by reduction with borane in THF.[44] However, in our hands this reaction failed. Other attempts to prepare **19** involving Wolff−Kishner reduction of donepezil or benzylation of piperidine **13** afforded intractable mixtures containing the desired product together with starting materials and some byproduct, as those arising from demethylation of the 5-methoxy group, in the first case, or from *N*,*N*-dibenzylation, in the latter. Finally, we prepared **19** in 53% yield by $NaBH_3CN$ reductive alkylation of piperidine **13** with benzaldehyde (Scheme 2), followed by purification by silica gel column chromatography.

The novel hybrids **14**−**17a**,**b** were fully characterized as dihydrochlorides through their spectroscopic data and elemental analyses (C, H, N, Cl), while the known indane analogue of donepezil **19** was characterized by spectroscopic data and HRMS analyses.

Pharmacology

AChE and BChE Inhibition. To determine the potential interest of the new donepezil−tacrine hybrids **14**−**15a**,**b** and the indane derivatives **16**−**17a**,**b** for the treatment of AD, their AChE inhibitory activity was assayed by the method of Ellman et al.[47] on AChE from bovine (bAChE) and human (hAChE) erythrocytes. Recent evidence has shown that in advanced AD patients, AChE activity is greatly reduced in specific brain regions while BChE activity increases, likely as compensation for AChE decrease.[48] The increasing role of BChE in the hydrolysis of acetylcholine as the ratio AChE/BChE gradually decreases in these patients suggests that inhibition of BChE might be valuable in the search for anti-Alzheimer agents.[48,49] Consequently, the inhibitory activity on human serum BChE (hBChE) was also assayed by the same method.

Table 1. Pharmacological Data of the Hydrochlorides of Tacrine, 6-Chlorotacrine, Donepezil, Compound **19**, and the Dihydrochlorides of the Donepezil−Tacrine Hybrids **14**−**15a,b** and Their Indane Derivatives **16**−**17a**,**b**[a]

	IC_{50} (nM)		
compd	bAChE	hAChE	hBChE
14a·2HCl	1.74 ± 0.02	4.04 ± 0.06	12.4 ± 0.6
14b·2HCl	0.29 ± 0.03	0.88 ± 0.04	12.3 ± 0.6
15a·2HCl	0.57 ± 0.05	0.67 ± 0.06	136 ± 9
15b·2HCl	0.09 ± 0.01	0.27 ± 0.03	66.3 ± 4.0
16a·2HCl	2.28 ± 0.06	5.13 ± 0.52	8.06 ± 0.32
16b·2HCl	0.82 ± 0.06	2.16 ± 0.21	7.25 ± 0.33
17a·2HCl	1.86 ± 0.07	2.60 ± 0.23	88.7 ± 0.2
17b·2HCl	0.82 ± 0.08	1.06 ± 0.05	72.7 ± 4.2
tacrine·HCl	130 ± 10	205 ± 18	43.9 ± 1.7
6-chlorotacrine·HCl	5.73 ± 0.44	8.32 ± 0.75	916 ± 19
donepezil·HCl	8.12 ± 0.26	11.6 ± 1.6	7273 ± 621
19·HCl	1451 ± 33	not determined	6401 ± 119

[a] Values are expressed as mean ± standard error of the mean of at least four experiments. IC_{50} inhibitory concentration (nM) of AChE (from bovine or human erythrocytes) or BChE (from human serum) activity.

Table 1 summarizes the data for the new compounds, as well as for tacrine·HCl, 6-chlorotacrine·HCl, and donepezil·HCl as reference compounds. Although the indane analogue of donepezil **19** is a known compound,[44] its biological activity has not been determined. In order to extend the comparison of activity between indanone and indane derivatives planned for the novel hybrids, the cholinesterase inhibitory activity of this indane derivative of donepezil was also assessed. All of the new hybrids are highly potent bAChE inhibitors, exhibiting IC_{50} values in the subnanomolar range in most cases and being clearly more potent than the parent compounds tacrine (57- to 1440-fold), 6-chlorotacrine (3- to 65-fold), donepezil (4- to 90-fold), and **19** (640- to 16100-fold). Hybrids **14**−**15**, which bear the indanone system of donepezil, are more potent bAChE inhibitors (1.3- to 9-fold more potent) than their indane analogues **16**−**17**, although the difference is much more pronounced in the case of donepezil and **19** (180-fold). The presence of a chlorine atom in the tacrine moiety enhances the inhibitory potency by 3-fold in indanone hybrids, while it has less effect in indane hybrids. Moreover, the three-methylene tether in the hybrids of the **b** series makes them 6- and 3-fold more potent than their indanone and indane counterparts of the **a** series, respectively. Overall, compound **15b** is the most active compound with an IC_{50} of 90 pM.

The new hybrids result in less potent inhibitors of human than bovine AChE (1.2- to 3-fold less potent), as it is the case for the parent compounds (around 1.5-fold less potent). Nevertheless, they are highly potent hAChE inhibitors, being more active than tacrine (40- to 760-fold), 6-chlorotacrine (2-to 30-fold), and donepezil (2- to 45-fold). As observed for bAChE, the best substitution pattern involves the presence of a chlorine atom at position 6 of the tacrine unit, the indanone ring of donepezil, and a tether length of three methylenes. As a result, **15b** is also the most active hAChE inhibitor (IC_{50} = 0.27 nM).

Moreover, the new hybrids are potent inhibitors of hBChE, though their activity is lower than that shown for hAChE. Thus, these compounds are 1.6- to 246-fold more potent toward hAChE than hBChE, as it is found for 6-chlorotacrine and donepezil (110- and 627-fold more potent toward AChE) but in contrast with tacrine (4.7-fold more potent toward BChE). When hBChE inhibitory activity is considered, the structure−activity relationships in this novel class of compounds reveal trends different from those observed for the AChE inhibitory activity. Thus, the indane hybrids **16**−**17** are 1.5-fold more potent than their analogues **14**−**15** bearing the indanone system of donepezil

(with the only exception of **17b**, which is slightly less potent than **15b**), which agrees with the 1.1-fold increase in potency of indane analogue **19** relative to donepezil. Moreover, a chlorine atom at position 6 of the tacrine unit is detrimental for the hBChE inhibitory activity, the unsubstituted hybrids **14** and **16** being 10-fold more potent than their 6-chloro derivatives **15** and **17**, which agrees with the 21-fold increase in potency of tacrine relative to 6-chlorotacrine and with the results reported for other tacrine-based dual binding site AChE inhibitors.[12,26] The effect of the tether length on the BChE inhibitory activity is much lower than that observed when the AChE inhibitory activity is considered, the hybrids of the **b** series being equipotent or slightly more potent (up to 2-fold) than their counterparts of the **a** series. Overall, the most active BChE inhibitor is **16b** (IC_{50} = 7.25 nM), which is 6-, 125-, 1000-, and 880-fold more potent than tacrine, 6-chlorotacrine, donepezil, and **19**, respectively.

Although the higher AChE vs BChE inhibitory activity of the first tacrine-based homo- and heterodimers was initially ascribed to the lack of a peripheral binding site in BChE,[1,46] recent studies have suggested that Phe278 would be responsible for $\pi-\pi$ interactions with aromatic moieties of tacrine-based heterodimers.[28] The higher BChE inhibitory activity of bis(7)-tacrine and several tacrine-based heterodimers,[28,29] as well as that of some of the new donepezil−tacrine hybrids herein described, relative to tacrine seems to validate this hypothesis. At this point, the high inhibitory activity toward both AChE and BChE of most of the donepezil−tacrine hybrids should not be detrimental for an anti-Alzheimer agent because dual inhibition of AChE and BChE could increase the efficacy of treatment and broaden the indications.[49]

The novel compounds reported in this study compare quite favorably with the previously known donepezil−tacrine hybrids.[30,31] Thus, hybrids **14**−**17a**,**b** are more potent AChE inhibitors than compounds **3** (IC_{50} = 6.0 nM, using rat cortex AChE; IC_{50} = 223 and 5.7 nM[21] for tacrine and donepezil, respectively, with the same enzyme source) and **4** (IC_{50} = 25 nM, using bovine erythrocyte AChE; IC_{50} = 167 and 19 nM for tacrine and donepezil, respectively, in the same assay). Regarding the BChE inhibitory activity, compounds **14a**,**b** and **16a**,**b** are more potent than **3** (IC_{50} = 76 nM, using rat serum BChE; IC_{50} = 92 and 7138 nM[21] for tacrine and donepezil, respectively, with the same enzyme source), though none of them is as potent as **4** (IC_{50} = 0.6 nM, using hBChE; IC_{50} = 24 and 930 nM for tacrine and donepezil, respectively).

Thioflavin T Competition Assay. Inestrosa et al. reported that AChE binds, through its peripheral site, to Aβ, thereby inducing amyloid fibril formation,[20,50,51] thus making blockade of the AChE peripheral site an interesting pharmacological target to develop disease-modifying anti-Alzheimer drug candidates. Since propidium, a selective inhibitor of the AChE peripheral site, exhibits an increase in fluorescence upon binding to AChE, it has been used as a probe for competitive ligand binding to the enzyme.[31,52,53] Thioflavin T is another fluorescent probe widely used to detect amyloid structures,[54] though it can also bind to other proteins.[55,56] In particular, thioflavin T binds to the AChE peripheral site, and the fluorescence enhancement reported for thioflavin T upon binding to AChE is much greater than that observed with propidium.[56] Therefore, we chose thioflavin T to study the interaction of selected donepezil−tacrine hybrids (compounds **15a** and **15b**) at the AChE peripheral site.

Table 2 shows the reduction of thioflavin T fluorescence arising from the competition with **15a** and **15b**, as well as tacrine, 6-chlorotacrine, and donepezil as reference compounds.

Table 2. Thioflavin T Competition Assay Results with the Dihydrochlorides of the Donepezil−Tacrine Hybrids **15a** and **15b** and with the Hydrochlorides of Tacrine, 6-Chlorotacrine, and Donepezil[a]

compd	reduction of fluorescence (%)
15a·2HCl	79.4 ± 3.5
15b·2HCl	57.0 ± 2.0
tacrine·HCl	12.6 ± 3.8
6-chlorotacrine·HCl	12.4 ± 1.9
donepezil·HCl	26.0 ± 3.5

[a] Percentage of thioflavin T fluorescence reduction by effect of several AChE inhibitors at 100 μM concentration. Values are expressed as the mean ± standard error of the mean of three experiments.

Table 3. Inhibition of hAChE-Induced Aggregation of Aβ_{1-40} by Donepezil−Tacrine Hybrids **15**−**17a**,**b** and Tacrine, 6-Chlorotacrine, Donepezil, and **19** as Reference Compounds[a]

compd	inhibition at 100 μM ± SEM (%)
15a·2HCl	37.6 ± 8.8
15b·2HCl	46.1 ± 9.0
16a·2HCl	60.0 ± 3.2
16b·2HCl	65.9 ± 2.5
17a·2HCl	61.6 ± 1.8
17b·2HCl	63.5 ± 6.2
tacrine·HCl	7[b]
6-chlorotacrine·HCl	8.5 ± 1.6
donepezil·HCl	22[b]
19·HCl	17.5 ± 2.5

[a] Values are the mean of two independent measurements, each performed in duplicate (SEM = standard error of the mean). [b] Data from ref 23.

Since the excitation wavelength of propidium is very close to the emission wavelength of thioflavin T, this compound was not included in the assay. The active site inhibitors tacrine and 6-chlorotacrine reduce thioflavin T fluorescence, on average, by 12%, an effect that might be ascribed to changes in the local conformation at the peripheral site induced upon binding at the AChE active site.[56] The dual binding site AChE inhibitor donepezil led to a 2-fold greater reduction in fluorescence (26% reduction) relative to the preceding active site inhibitors, as expected from the direct interaction of the indanone moiety with the AChE peripheral site. Finally, the novel donepezil−tacrine hybrids **15a** and **15b** produced the highest reductions in thioflavin T fluorescence among all the tested compounds (79% and 57% reduction, respectively), which could be ascribed to the displacement of the fluorophore at the peripheral site of the enzyme. Moreover, the 3- and 2-fold greater effect obtained for **15a** and **15b** relative to donepezil suggests a larger occupancy of the AChE peripheral site by the indanone unit of the novel hybrids.

Inhibiton of AChE-Induced Aβ Aggregation. The results of the thioflavin T competition assay provide indirect evidence of the ability of these donepezil−tacrine hybrids to interfere with the AChE-induced Aβ aggregation. A direct measure involving AChE and Aβ was therefore required to assess the potential disease-modifying role of these hybrids. Thus, the inhibitory activity of hybrids **15**−**17a**,**b** on the AChE-induced aggregation of Aβ_{1-40} was determined by a thioflavin T fluorescent method.[23] Also, the Aβ-antiaggregating effect of 6-chlorotacrine and the indane derivative of donepezil **19** was determined, while those of tacrine and donepezil were already described.[23]

Table 3 summarizes the Aβ-antiaggregating activity of the novel hybrids and reference compounds. The six tested donepezil−tacrine hybrids exhibit, at a 100 μM concentration, a significant Aβ-antiaggregating effect with percentages of inhibition ranging from 38% to 66%, being 5.4- to 9.4-fold more potent than tacrine, 4.4- to 7.8-fold more potent than 6-chlorotacrine, 1.7- to 3-fold more potent than donepezil, and 2.1-

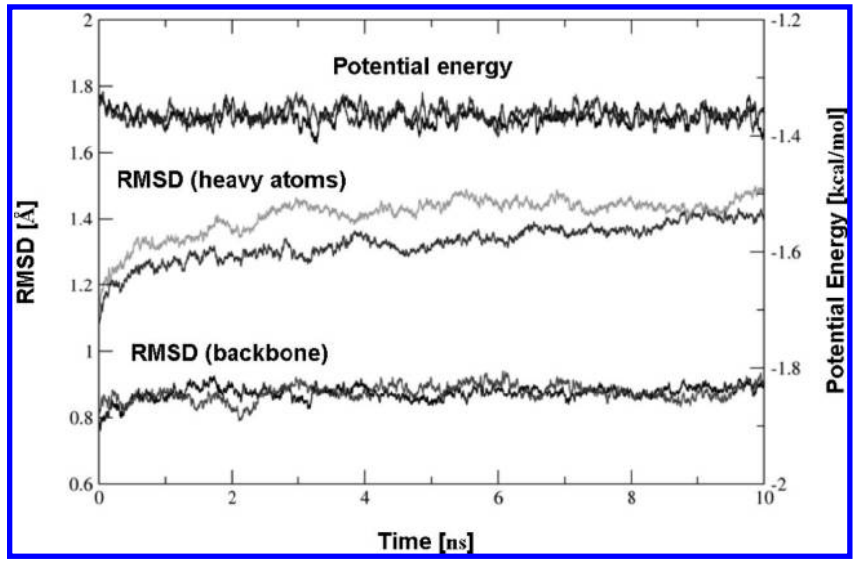

Figure 1. Time dependence of the potential energy ($\times 10^5$, kcal/mol) and the positional root-mean-squared deviation (rmsd, Å) determined for the backbone and heavy atoms in the mobile part of the simulation system for the hAChE complexes with **15a** (gray) and **15b** (black). The profiles were smoothed in 50 ps windows for the sake of clarity.

to 3.8-fold more potent than **19**. Indane derivatives **16**−**17a**,**b** are clearly more potent than indanone derivatives **15a**,**b** (about 1.5-fold), in contrast with the similar effect determined for donepezil and its indane derivative **19**. The length of the linker and the substitution at the active site interacting unit, i.e., the presence or absence of the chlorine atom at position 6 of the tacrine unit, have little effect on the Aβ-antiaggregating activity of the hybrids, observing only a slightly increased effect in the hybrids bearing the trimethylene linker. The Aβ-antiaggregating effects exhibited by these donepezil−tacrine hybrids are in the same range as those of known dual binding site AChE inhibitors such as lipocrine,[11] xanthostigmine derivatives,[13] and bis-(7)-tacrine derivatives,[17] while other families with lower[9,14] or higher[10,12,15,16] potencies have been developed.

The ability of dual binding site AChE inhibitors to block the AChE-induced Aβ aggregation constitutes their most interesting property because of the derived potential to interfere upstream in the neurotoxic cascade of AD. However, some concerns exist about the biological relevance of the results of the in vitro Aβ antiaggregating effects of these compounds. Indeed, these assays are performed using much higher concentrations of AChE and Aβ than those present in brain, but they are necessary to accelerate the aggregation process up to a reasonable extent for analytical purposes. Also, the concentration of inhibitor used in these assays is much higher (usually 100 μM) than those necessary to inhibit AChE (in the nanomolar or picomolar range). However, as pointed out elsewhere,[23] these high concentration values should be normalized in order to compare the inhibition data. Thus, if the inhibitor/AChE concentration ratio in both the Ellman's assay for determination of the AChE inhibitory activity and in the thioflavin T-based fluorometric assay for determination of the Aβ antiaggregating effect is taken into account, the resulting values are indeed of the same magnitude. Thus, it would seem reasonable that similar amounts of a given inhibitor might afford both inhibitory activities.

Moreover, the proof-of-concept of the therapeutic usefulness of the in vitro Aβ antiaggregating effect of dual binding site AChEIs has been recently obtained in in vivo studies. Thus, memoquin, a dual binding site AChEI that in vitro blocked by 87% the AChE-induced Aβ aggregation at 100 μM,[15,16] has been shown to delay Aβ expression to significantly reduce Aβ deposits and to rescue behavioral deficits linked to attention and memory in 15-month-old AD11 mice, a kind of transgenic mice that display a full set of hallmarks of AD.[15] Also, Neuropharma's NP-61 (formerly NP-0361), a dual binding site AChEI that in vitro inhibited the AChE-induced Aβ aggregation with an IC_{50} value 1 order of magnitude lower than that of propidium, reduced the number, surface area, and size of amyloid plaques in the cortex and hippocampus in human amyloid precursor protein (hAPP) transgenic mice (Swedish and London mutation) after oral administration during 3 months, and the reduced brain amyloid burden resulted in a significantly increased cognition (spatial learning and memory in the Morris water maze test).[57] In the first half of 2007, NP-61 entered phase I clinical trials for Alzheimer's disease in the U.K.,[58] which constitutes clear evidence of the promising role of these compounds as anti-Alzheimer disease-modifying agents.

Molecular Modeling Studies

To gain insight into the molecular determinants that modulate the inhibitory activity of the novel donepezil−tacrine hybrids, the binding modes of **15a** and **15b** were explored by means of 10 ns molecular dynamics (MD) simulations performed for their complexes to hAChE. In the two cases the potential energy dropped smoothly during the first nanosecond, but it remained nearly constant for the rest of the trajectory (Figure 1). Indeed, the stability of the trajectories is supported by the small positional root-mean-squared deviations determined for the backbone and heavy atoms, which amount to around 0.9 and 1.4 Å, respectively (Figure 1).

The position of **15a** with respect to selected key residues in the binding site is shown in Figure 2. The tacrine moiety is firmly bound to the catalytic site of hAChE, it being stacked against the aromatic rings of Trp86 and Tyr337 (average distances from the central ring of tacrine of 3.73 and 4.35 Å, respectively, and numbering of residues corresponding to hAChE). The aromatic nitrogen of tacrine, protonated at physiological pH, is hydrogen-bonded to the main chain carbonyl oxygen of His447 (average N···O distance of 2.81 Å). Finally, the chlorine atom occupies a small hydrophobic pocket formed by Trp439, Met443, and Pro446, which parallels the interaction observed between the chlorine atom at position 3 of huprine X, a hybrid compound whose structure contains a

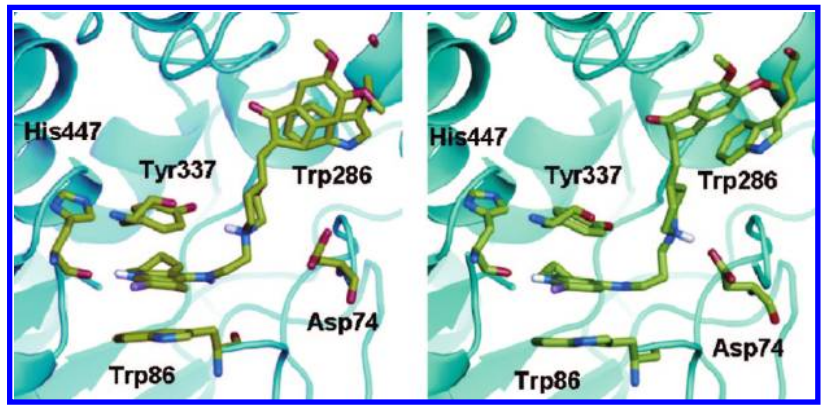

Figure 2. Representation of the heterodimers **15a** (left) and **15b** (right) in the binding site of hAChE highlighting selected residues that form the main interactions with tacrine, piperidine, and indanone units of the inhibitors. Most hydrogen atoms are omitted for the sake of clarity.

6-chlorotacrine moiety, and *Tc*AChE,[38,59] though in this latter case Pro446 is replaced by Ile439. The occupancy of such hydrophobic pocket by the chlorine atom contributes to the higher potency of heterodimers having the 6-chlorotacrine unit relative to their unsubstituted counterparts. As noted previously,[12,28] in hBChE, Met437 replaces Pro446 of hAChE and Ile439 of *Tc*AChE, which makes the terminal methyl group of Met437 to be around 1.2 Å closer to the chlorine atom. The larger steric hindrance due to the greater proximity of the chlorine atom to Met437 could account for the detrimental influence of this substituent on the hBChE inhibitory activity.

Regarding the linker, which is aligned along the gorge, the most relevant features come from the interactions formed by the piperidine ring. This unit occupies a position slightly shifted from that found in the X-ray crystallographic structure of the *Tc*AChE-donepezil complex (PDB entry 1EVE), although it still retains the electrostatic interaction with the carboxylate group of Asp74 (average N(piperidine)···O(carboxylate) distance of 4.72 Å). In turn, this latter residue is hydrogen-bonded to the hydroxyl group of Tyr72 (average O···O distance of 2.87 Å). Moreover, the protonated piperidine nitrogen is hydrogen-bonded to the hydroxyl group of Tyr337 (average N(piperidine)···O distance of 3.20 Å). Thus, a network of interactions that couple several residues in the gorge and the catalytic binding site is formed. Finally, the indanone ring is stacked onto the aromatic ring of Trp286 (average distance between the centers of indanone and indole rings of 4.38 Å), whose orientation resembles that found in the *Tc*AChE−donepezil complex. Moreover, the carbonyl group of the indanone unit forms water-mediated contacts with the backbone N−H groups of Phe295 and Arg296 and the C═O groups of Pro290 and Ser293, which should contribute to the higher AChE inhibitory activity of indanone derivatives relative to the indane analogues.

The binding mode of **15b** at the catalytic site of hAChE closely mimics the interactions noted above for **15a** (Figure 2). Thus, the tacrine ring is stacked against Trp86 and Tyr337 (average distances between rings of 3.63 and 4.44 Å, respectively), the protonated quinoline nitrogen is hydrogen-bonded to the main chain carbonyl oxygen of His447 (average N···O distance of 2.82 Å), and the chlorine atom fills the hydrophobic pocket formed by Trp439, Met443, and Pro446. The enlargement of the tether length, however, leads to differences in the interactions found along the gorge and at the peripheral site. First, the protonated piperidine N−H group points directly to the carboxylate group of Asp74 (average N···O distance of 2.73 Å), which would strengthen the electrostatic interaction. The hydrogen bonds between Asp74 and Tyr72 and between the piperidine N−H unit and Tyr337 observed in the binding of **15a** are lost in the complex with **15b**. Thus, Asp74 forms a hydrogen-bond interaction with the backbone N−H unit of Leu76 and the hydroxyl group of Tyr337 establishes a hydrogen-bond contact with Tyr124. Second, though at the beginning of the simulation the indanone ring was stacked onto the indole ring of Trp286, its orientation changed along the first nanosecond of MD simulation and adopted an arrangement roughly normal to the indole ring (Figure 3). This change was accompanied by a conformational change in the indole ring of Trp286, whose position differed from that found in the X-ray structure by a rotation around the $C_\alpha-C_\beta-C3_{indole}-C3a_{indole}$ from −83° (in 1EVE) to +32°. This finding, therefore, supports the conformational plasticity of this residue in the peripheral site of the enzyme already noted by other studies.[12,60–62]

Comparison of the binding mode of compounds **15a** and **15b** with that of tacrine and donepezil (taken from X-ray structures 1ACJ and 1EVE, respectively) shows that the tacrine unit in the dual binding site inhibitors closely matches the position occupied by tacrine in the catalytic site (Figure 4). There are, however, notable differences in the relative arrangement of the indanone units of **15a** and **15b**. Thus, in **15a** this unit is shifted compared to the position occupied by the corresponding moiety of donepezil, leading to a more efficient $\pi-\pi$ stacking interaction between the indanone ring of **15a** and the indole ring of Trp286 (Figure 4). In **15b** the strong electrostatic interaction formed between the protonated piperidine and Asp74 explains the distinct orientation of the indanone unit relative to donepezil and the conformational change adopted by the indole ring of Trp286, which impedes the formation of a $\pi-\pi$ stacking interaction (Figure 4).

Conclusion

We have synthesized a new series of donepezil−tacrine hybrids, designed to simultaneously interact with the active, peripheral, and mid-gorge binding sites of AChE. In contrast to previous approaches, the conjunctive strategy adopted here largely preserves the chemical skeleton of donepezil while its benzyl moiety is replaced by a tacrine unit. The length of the tether that connects the two constituting fragments of the novel hybrids, i.e., the 5,6-dimethoxy-2-[(4-piperidinyl)methyl]-1-indanone moiety of donepezil (or its corresponding indane derivative) and the tacrine (or 6-chlorotacrine) unit, has a relevant effect on the arrangement of the hybrid along the gorge, leading to different orientations of the piperidine ring and the indanone system within the enzyme gorge and at the peripheral site, respectively, while their tacrine unit closely matches the position occupied by tacrine within the AChE active site. Thus,

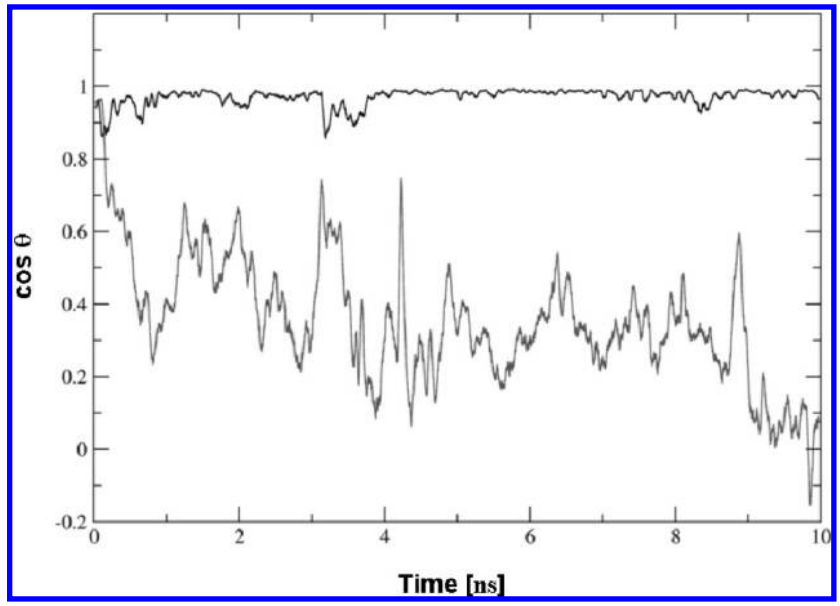

Figure 3. Time dependence of the relative orientation of the indanone ring of heterodimers **15a** (black) and **15b** (gray) and the indole ring of Trp286 at the peripheral site. The relative orientation was measured from the cosine function of the angle formed by the vectors normal to the indanone and indole rings. Accordingly, a perfect stacking would correspond to cos $\theta = 1$, while a perpendicular arrangement is denoted by cos $\theta = 0$.

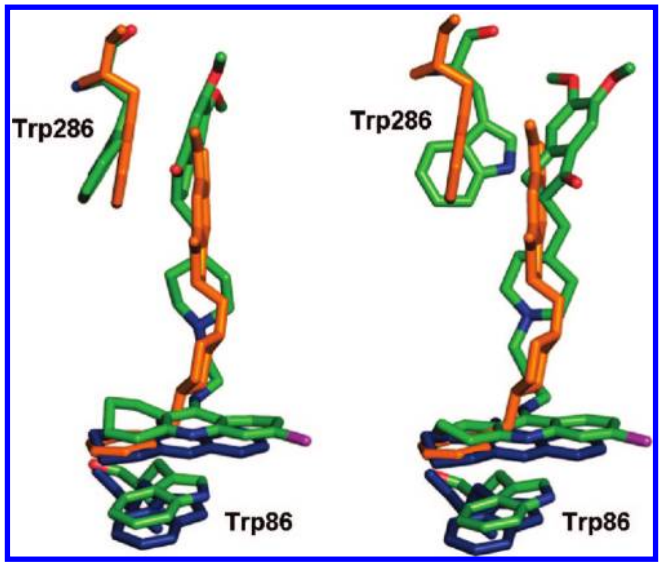

Figure 4. Superposition of the heterodimers **15a** (left) and **15b** (right) with tacrine (taken from the 1ACJ X-ray structure of the *Tc*AChE−tacrine complex, blue) and donepezil (from the 1EVE X-ray structure of the *Tc*AChE−donepezil complex, orange), showing the relative positions of Trp86 (Trp84 in 1ACJ) and Trp286 (Trp279 in 1EVE) at the catalytic and peripheral sites, respectively. Compounds **15a** and **15b** are colored by atom.

enlargement of the linker from two to three methylenes permits the piperidine ring to form a direct electrostatic interaction with Asp74, though at the expense of a less efficient $\pi-\pi$ interaction between the indanone unit and the indole ring of Trp286. In spite of these structural differences, all of the new hybrids are highly potent bovine and human AChE inhibitors, exhibiting IC_{50} values in the subnanomolar range in most cases and being clearly more potent than the parent compounds from which they were designed and the previously described donepezil−tacrine hybrids. The most potent AChE inhibitors are those bearing an indanone system, a chlorine atom at the tacrine unit and a tether length of three methylenes. Though all of the new hybrids are less potent toward hBChE, the most active compounds, i.e., those bearing an unsubstituted tacrine unit irrespective of the presence of an indanone or indane system and the tether length, are also more potent hBChE inhibitors than the parent compounds. Following some interesting results arising from a thioflavin T competition assay to assess their interaction with the AChE peripheral site, six out of the eight hybrids of the series were tested for their ability to block the AChE-induced Aβ-aggregation. All the tested hybrids exhibited a significant Aβ antiaggregating activity, being more potent than the parent compounds, including the dual binding site inhibitor donepezil. Overall, these results suggest that the novel donepezil−tacrine hybrids herein reported may have a potential disease-modifying role in the treatment of AD.

Experimental Section

Chemistry. General Methods. Melting points were determined in open capillary tubes with a MFB 595010 M Gallenkamp melting point apparatus. The 300 MHz ^{1}H/75.4 MHz ^{13}C NMR spectra, 400 MHz ^{1}H/100.6 MHz ^{13}C NMR spectra, and 500 MHz ^{1}H NMR spectra were recorded on Varian Gemini 300, Varian Mercury 400, and Varian Inova 500 spectrometers, respectively. The chemical shifts are reported in ppm (δ scale) relative to internal tetramethylsilane, and coupling constants are reported in hertz (Hz). Assignments given for the NMR spectra of the new compounds have been carried out by comparison with the NMR data of **15a**, **16a**, **17b**, and 6-chlorotacrine, as model compounds, which in turn were assigned on the basis of DEPT, COSY ^{1}H/^{1}H (standard procedures), NOESY ^{1}H/^{1}H, and COSY ^{1}H/^{13}C (gHSQC and gHMBC sequences) experiments. IR spectra were run on a Perkin-Elmer Spectrum RX I spectrophotometer. Absorption values are expressed as wavenumbers (cm^{-1}); only significant absorption bands are given. Column chromatography was performed on silica gel 60 AC.C (35−70 mesh, SDS, no. 2000027). Thin-layer chromatography was performed with aluminum-backed sheets with silica gel 60 F_{254} (Merck, no. 1.05554), and spots were visualized with UV light and 1% aqueous solution of $KMnO_4$. Analytical grade solvents were used for crystallization, while pure for synthesis solvents were used in the reactions, extractions, and column chromatography. For characterization purposes, the new donepezil−tacrine hybrids were transformed into the corresponding dihydrochlorides and recrystallized. Worthy of note, as previously reported for some tacrine-related dimeric compounds,[63] the new donepezil−tacrine

hybrids have the ability to retain molecules of water, which cannot be removed after drying the analytical samples at 80 °C/30 Torr for 2 days. Thus, the elemental analyses of these compounds showed the presence of variable amounts of water. NMR spectra of all of the new compounds were performed at the Serveis Científico-Tècnics of the University of Barcelona, while elemental analyses and high resolution mass spectra were carried out at the Microanalysis Service of the IIQAB (CSIC, Barcelona, Spain) with a Carlo Erba model 1106 analyzer and at the Mass Spectrometry Laboratory of the University of Santiago de Compostela (Spain) with a Micromass Autospec spectrometer, respectively.

General Procedure for the Reaction of 9-Chloro-1,2,3,4-tetrahydroacridine, 5, or 6,9-Dichloro-1,2,3,4-tetrahydroacridine, 6, with ω-Aminoalcohols. A mixture of **5** or **6** (1 mmol) and an excess of the aminoalcohol **7** (3 mmol) in 1-pentanol (1 mL) was heated under reflux with magnetic stirring for 18 h. The resulting mixture was cooled to room temperature, diluted with AcOEt (5 mL), and extracted with 1 N HCl (4 × 3 mL). The combined aqueous extracts were washed with AcOEt (3 × 3 mL), alkalinized with NaOH pellets (until pH 12), and extracted with CH_2Cl_2 (3 × 8 mL). The combined organic extracts were dried with anhydrous Na_2SO_4 and concentrated in vacuo to give alcohol **8** or **9** as a pale-brown solid or oily residue, which was used in the next step without further purification.

For characterization purposes, analytical samples of the hydrochlorides of **8** and **9** were prepared as follows: The alcohol **8** or **9** (1 mmol) was dissolved in MeOH (10 mL). The solution was filtered through a 0.45 μm polytetrafluoroethylene (PTFE) filter and treated with an excess of a methanolic solution of HCl (3 mmol), and the resulting solution was concentrated in vacuo to dryness. The solid was recrystallized from a mixture MeOH/AcOEt in a ratio of 1:4 (5 mL) and dried at 80 °C/30 Torr for 48 h to give the 9-(ω-hydroxyalkylamino)tetrahydroacridine hydrochloride **8**·HCl or **9**·HCl as a light-brown solid.

9-[(2-Hydroxyethyl)amino]-1,2,3,4-tetrahydroacridine Hydrochloride (8a·HCl). From **5** (3.34 g, 15.4 mmol) and 2-aminoethanol **7a** (2.48 mL, 2.83 g, 46.4 mmol), alcohol **8a** (3.52 g, 95% yield, free base) was obtained: R_f = 0.38 (CH_2Cl_2/MeOH/25% aqueous NH_4OH, 9:1:0.1). **8a**·HCl: mp 184−185 °C (MeOH/AcOEt, 1:4); IR (KBr) ν 3700−2400 (max at 3358, 3142, 3058, 3016, 2938, 2872, O−H, N−H, $^+$N−H, and C−H st), 1633, 1592, 1577, and 1524 (ar−C−C and ar−C−N st) cm^{-1}; ^{1}H NMR (300 MHz, CD_3OD) δ 1.90−2.04 (complex signal, 4H, 2-H_2 and 3-H_2), 2.74 (m, 2H, 1-H_2), 3.01 (m, 2H, 4-H_2), 3.86 (t, J = 5.4 Hz, 2H, 2′-H_2), 4.01 (t, J = 5.4 Hz, 2H, 1′-H_2), 4.87 (s, OH, NH and $^+$NH), 7.54 (ddd, J = 8.4 Hz, J' = 6.0 Hz, J'' = 2.4 Hz, 1H, 7-H), 7.76−7.84 (complex signal, 2H, 5-H and 6-H), 8.40 (d, J = 8.4 Hz, 1H, 8-H); ^{13}C NMR (75.4 MHz, CD_3OD) δ 21.1 (CH_2, C3), 23.1 (CH_2, C2), 24.8 (CH_2, C1), 30.1 (CH_2, C4), 51.2 (CH_2, C1′), 61.7 (CH_2, C2′), 113.7 (C, C9a), 117.7 (C, C8a), 121.2 (CH, C5), 126.0 (CH, C8), 126.1 (CH, C7), 133.3 (CH, C6), 140.9 (C, C10a), 152.8 (C, C4a), 157.4 (C, C9). HRMS calcd for ($C_{15}H_{18}N_2O$ + H^+) 243.1497, found 243.1494.

General Procedure for the Mesylation of Alcohols 8 and 9. To a cold solution (−10 °C, ice−salt bath) of the alcohol **8** or **9** (1 mmol) and anhydrous Et_3N (1.7 mmol) in anhydrous CH_2Cl_2 (6 mL), methanesulfonyl chloride (1.5 mmol) was added dropwise, and the reaction mixture was stirred for 30 min at this temperature. The mixture was concentrated in vacuo, the residue was taken in CH_2Cl_2 (4 mL), and the resulting organic solution was washed with 2 N NaOH (3 × 3 mL) until the aqueous phase remained basic (pH > 10), dried with anhydrous Na_2SO_4, and concentrated in vacuo to give the corresponding mesylate **10** or **11** as a brown oily residue, which was used in the next step without further purification.

For characterization purposes, analytical samples of the mesylates were obtained by extraction of the oily crude product with hot AcOEt except in the case of **11a**, whose analytical sample was prepared by recrystallization of the corresponding hydrochloride, obtained in a similar way to that described for the hydrochlorides of alcohols **8** and **9**.

9-[(2-Methanesulfonyloxyethyl)amino]-1,2,3,4-tetrahydroacridine (10a). From alcohol **8a**(3.52 g, 14.5 mmol), mesylate **10a** (4.41 g, 95% yield) was obtained: R_f = 0.67 (CH_2Cl_2/MeOH/25% aqueous NH_4OH, 9:1:0.1); IR (NaCl) ν 3391 and 3339 (N−H st), 1638, 1586, and 1524 (ar−C−C and ar−C−N st), 1352 (SO_2 st as), 1178 (SO_2 st s) cm^{-1}; ^{1}H NMR (300 MHz, $CDCl_3$) δ 1.88−1.98 (complex signal, 4H, 2-H_2 and 3-H_2), 2.76 (m, 2H, 1-H_2), 2.97 (s, 3H, OSO_2CH_3), 3.08 (m, 2H, 4-H_2), 3.81 (m, 2H, 1′-H_2), 4.34 (t, J = 4.9 Hz, 2H, 2′-H_2), 4.54 (broad s, 1H, NH), 7.39 (ddd, J = 8.4 Hz, J' = 6.8 Hz, J'' = 1.5 Hz, 1H, 7-H), 7.57 (ddd, J = 8.4 Hz, J' = 6.8 Hz, J'' = 1.5 Hz, 1H, 6-H), 7.91−7.95 (complex signal, 2H, 5-H and 8-H); ^{13}C NMR (75.4 MHz, $CDCl_3$) δ 22.4 (CH_2) and 22.7 (CH_2) (C2 and C3), 24.7 (CH_2, C1), 33.3 (CH_2, C4), 37.3 (CH_3, OSO_2CH_3), 47.4 (CH_2, C1′), 69.0 (CH_2, C2′), 117.7 (C, C9a), 120.7 (C, C8a), 122.2 (CH), 124.3 (CH), 127.8 (CH), 128.7 (CH) (C5, C6, C7, and C8), 146.2 (C, C10a), 149.6 (C, C4a), 158.2 (C, C9). HRMS calcd for ($C_{16}H_{20}N_2O_3S$ + H^+) 321.127, found 321.128.

General Procedure for the Coupling of Mesylates 10 and 11 with 5,6-Dimethoxy-2-[(4-piperidinyl)methyl]indan-1-one (12) or 5,6-Dimethoxy-2-[(4-piperidinyl)methyl]indane (13). A solution of the mesylate **10** or **11** (1 mmol), the piperidine **12** or **13** (1 mmol), and anhydrous Et_3N (2.5 mmol) in DMSO (8 mL) was heated at 85 °C for 48 h. The resulting solution was allowed to cool to room temperature and was concentrated in vacuo. The brown oily residue was treated with aqueous 2 N NaOH (25 mL) and extracted with CH_2Cl_2 (3 × 35 mL). The combined organic extracts were washed with water (6 × 40 mL) and brine (4 × 30 mL), dried with anhydrous Na_2SO_4, filtered, and evaporated under reduced pressure to give an oily residue, which was submitted to column chromatography (35−70 μm silica gel, CH_2Cl_2/MeOH/25% aqueous NH_4OH mixtures as eluent).

The isolated donepezil−tacrine hybrids **14**−**17** were transformed into the corresponding dihydrochlorides as follows: A solution of the free base (1 mmol) in MeOH (40 mL) was filtered through a 0.45 μm PTFE filter and treated with excess of a methanolic solution of HCl (5 mmol). The solution was concentrated in vacuo to dryness, and the solid residue was recrystallized from MeOH (20 mL) and dried at 80 °C/30 Torr for 48 h.

9-[(2-{4-[(5,6-Dimethoxy-1-oxoindan-2-yl)methyl]piperidin-1-yl}ethyl)amino]-1,2,3,4-tetrahydroacridine Dihydrochloride (14a·2HCl). From mesylate **10a** (276 mg, 0.86 mmol) and piperidine **12** (249 mg, 0.86 mmol), compound **14a** (87 mg, 20% yield) was obtained as a pale-brown solid on elution with a mixture of CH_2Cl_2/MeOH/25% aqueous NH_4OH, 99.5:0.5:0.4: R_f = 0.91 (CH_2Cl_2/MeOH/25% aqueous NH_4OH, 90:10:0.1). **14a**·2HCl: mp 190−191 °C (MeOH); IR (KBr) ν 3700−2400 (max at 3401, 2928, 2871, 2718, N−H, $^+$N−H, and C−H st), 1685, 1672 (C═O st), 1636, 1588, 1523, and 1500 (ar−C–C and ar−C–N st) cm^{-1}; ^{1}H NMR (500 MHz, CD_3OD) δ 1.45 (m, 1H, indanone-2-CH_a), 1.62−1.73 (broad signal, 2H, piperidine 3-H_{ax} and 5-H_{ax}), 1.86 (m, 1H, indanone-2-CH_b), 1.90−2.02 (broad signal, 1H, piperidine 4-H), superimposed 1.99 (complex signal, 4H, acridine 2-H_2 and 3-H_2), 2.02 (broad d, J = 14.5 Hz, 1H) and 2.14 (broad d, J = 14.0 Hz, 1H) (piperidine 3-H_{eq} and 5-H_{eq}), 2.74−2.80 (complex signal, 2H, indanone 2-H and 3-H_a), 2.84 (m, 2H, acridine 1-H_2), 3.08 (m, 2H, acridine 4-H_2), 3.12 (broad signal, 2H, piperidine 2-H_{ax} and 6-H_{ax}), superimposed in part 3.34 (dd, J = 18.0 Hz, J' = 8.5 Hz, 1H, indanone 3-H_b), 3.60 (broad signal, 2H, $NHCH_2CH_2N$), 3.72 (broad signal, 2H, piperidine 2-H_{eq} and 6-H_{eq}), 3.85 (s, 3H, 6-OCH_3), 3.94 (s, 3H, 5-OCH_3), 4.42 (t, J = 7.7 Hz, 2H, $NHCH_2CH_2N$), 4.85 (s, NH and $^+$NH), 7.07 (s, 1H, indanone 4-H), 7.15 (s, 1H, indanone 7-H), 7.68 (ddd, J = 8.5 Hz, J' = 7.0 Hz, J'' = 1.0 Hz, 1H, acridine 7-H), 7.83 (dd, J = 8.5 Hz, J' = 1.0 Hz, 1H, acridine 5-H), 7.91 (ddd, J = 8.5 Hz, J' = 7.0 Hz, J'' = 1.0 Hz, 1H, acridine 6-H), 8.43 (d, J = 8.5 Hz, 1H, acridine 8-H); ^{13}C NMR (100.6 MHz, CD_3OD) δ 21.7 (CH_2, acridine C3), 23.0 (CH_2, acridine C2), 25.7 (CH_2, acridine C1), 29.5 (CH_2, acridine C4), 30.3 (CH_2) and 31.1 (CH_2) (piperidine C3 and C5), 33.0 (CH, piperidine C4), 34.2 (CH_2, indanone C3), 39.0 (CH_2, indanone-2-CH_2), 43.1 (CH_2, $NHCH_2CH_2N$), 46.1 (CH, indanone C2), 54.1 (2 CH_2, piperidine

C2 and C6), 56.5 (CH_3, 6-OCH_3), 56.7 (CH_3, 5-OCH_3), 57.4 (CH_2, $NHCH_2CH_2N$), 105.3 (CH, indanone C7), 109.0 (CH, indanone C4), 114.4 (C, acridine C9a), 117.6 (C, acridine C8a), 120.3 (CH, acridine C5), 125.9 (CH, acridine C8), 127.2 (CH, acridine C7), 129.8 (C, indanone C7a), 134.3 (CH, acridine C6), 139.4 (C, acridine C10a), 151.1 (C, indanone C6), 151.3 (C, indanone C3a), 153.1 (C, acridine C4a), 157.8 (C) and 158.0 (C) (indanone C5 and acridine C9), 209.7 (C, indanone C1). Anal. ($C_{32}H_{39}N_3O_3 \cdot 2HCl \cdot 1.5H_2O$) C, H, N, Cl.

Biochemical Studies. AChE inhibitory activity was evaluated spectrophotometrically at 25 °C by the method of Ellman,[47] using AChE from bovine or human erythrocytes and acetylthiocholine iodide (0.53 and 0.13 mM for bovine and human AChE, respectively) as substrate. The reaction took place in a final volume of 3 mL of 0.1 M phosphate-buffered solution, pH 8.0, containing 0.025 or 0.04 unit of bovine or human AChE, respectively, and 333 μM 5,5′-dithiobis(2-nitrobenzoic) acid (DTNB) solution used to produce the yellow anion of 5-thio-2-nitrobenzoic acid. Inhibition curves were performed in triplicate by incubating at least 12 concentrations of inhibitor for 15 min. One triplicate sample without inhibitor was always present to yield 100% of AChE activity. The reaction was stopped by the addition of 100 μL of 1 mM eserine, and the color production was measured at 414 nm. BChE inhibitory activity determinations were carried out similarly, using 0.035 unit of human serum BChE and 0.56 mM butyrylthiocholine, instead of AChE and acetylthiocholine, in a final volume of 1 mL.

Data from concentration−inhibition experiments of the inhibitors were calculated by nonlinear regression analysis, using the GraphPad Prism program package (GraphPad Software; San Diego, CA), which gave estimates of the IC_{50} (concentration of drug producing 50% of enzyme activity inhibition). Results are expressed as the mean ± SEM of at least four experiments performed in triplicate. DTNB, acetylthiocholine, butyrylthiocholine, and the enzymes were purchased from Sigma, and eserine was purchased from Fluka.

Thioflavin T Competition Assay. Fluorescence measurements were carried out at room temperature in a SFM-25 spectrofluorimeter (Biotek, Italy) using a 1 mL quartz cell. Fluorescence was monitored at 448 and 488 nm for excitation and emission, respectively. An aqueous solution of hAChE at 2.3 μM was stirred at room temperature for 24 h. After incubation, an amount of 50 μL of the enzyme solution was mixed with 750 μL of 50 mM glycine−NaOH buffer (pH 8.5) containing 15 μM thioflavin T. The resulting solution was stirred for 1 h, and the fluorescence of the sample was recorded (F_1). To check the ability of reducing the fluorescence arising from the interaction of AChE and thioflavin T, the enzyme, at a final concentration of 2.3 μM, was mixed with the inhibitor (final concentration of 100 μM), and the solution was stirred for 24 h. After incubation, an amount of 50 μL of the protein solution was mixed with 750 μL of fluorophore solution, as indicated above, and the corresponding fluorescence was recorded (F_2). Finally, the fluorescence of a solution formed by 750 μL of the buffer containing the dye and 50 μL of water was recorded (F_0). The percentage of reduction of ThT fluorescence was determined as

$$\% = 1 - \frac{F_2 - F_0}{F_1 - F_0} \quad (1)$$

Inhibition of AChE-Induced Aβ_{40} Aggregation Assay. Thioflavin T (Basic Yellow 1), human recombinant AChE lyophilized powder, and 1,1,1,3,3,3-hexafluoro-2-propanol (HFIP) were purchased from Sigma Chemicals. Buffers and other chemicals were of analytical grade. Absolute DMSO over molecular sieves was from Fluka. Water was deionized and doubly distilled. β-Amyloid 1−40 (Aβ_{40}), supplied as trifluoroacetate salt, was purchased from Bachem AG (Bubendorf, Switzerland). Aβ_{40} (2 mg mL^{-1}) was dissolved in HFIP and lyophilized. The 1 mM solutions of tested inhibitors were prepared by dissolution in MeOH.

Aliquots of 2 μL of Aβ_{40} peptide, lyophilized from 2 mg mL^{-1} HFIP solution and dissolved in DMSO, were incubated for 24 h at room temperature in 0.215 M sodium phosphate buffer (pH 8.0) at a final concentration of 230 μM. For co-incubation experiments, aliquots (16 μL) of hAChE (final concentration of 2.30 μM, Aβ/AChE molar ratio of 100:1) and AChE in the presence of 2 μL of the tested inhibitor (final inhibitor concentration 100 μM) in 0.215 M sodium phosphate buffer, pH 8.0, solution were added. Blanks containing Aβ_{1-40} alone, human recombinant AChE alone, and Aβ_{1-40} plus tested inhibitors in 0.215 M sodium phosphate buffer (pH 8.0) were prepared. The final volume of each vial was 20 μL. Each assay was run in duplicate. To quantify amyloid fibril formation, the thioflavin T fluorescence method was then applied.[23] The fluorescence intensities due to β-sheet conformation were monitored for 300 s at $\lambda_{em} = 490$ nm ($\lambda_{exc} = 446$ nm). The percent inhibition of the AChE-induced aggregation due to the presence of the tested compound was calculated by the following expression: $100 - [(IF_i/IF_o) \times 100]$ where IF_i and IF_o are the fluorescence intensities obtained for Aβ plus AChE in the presence and in the absence of inhibitor, respectively, minus the fluorescence intensities due to the respective blanks.

Molecular Modeling Methods. The binding modes of compounds **15a** and **15b** were explored by means of 10 ns molecular dynamics simulations performed for their complexes to human acetylcholinesterase (hAChE). To this end, models of the bonded ligands were built up using the X-ray crystallographic structure of the hAChE−fasciculin complex (PDB code 1B41).[64] Fasciculin was removed from the structure, truncated residues were reconstructed, and missing residues were modeled using InsightII graphics package.[65] The starting pose of the ligands was determined by means of docking computations with GOLD[66] (using GoldScore scoring function), which was successful for predicting the docking of donepezil in the enzyme (see Supporting Information), and was later refined by inspection of the X-ray crystallographic structures of the *Tc*AChE complexes with tacrine (1ACJ),[35] huprine X (1E66),[38] and donepezil (1EVE)[22] and the final structures of previous heterodimer studies.[12,31] The system was hydrated by centering a sphere of 50 Å of TIP3P[67] water molecules at the inhibitor, paying attention to filling the position of crystallographic waters inside the binding cavity. Finally, six Na^+ cations were added to neutralize the negative charge of the system with the xleap module of AMBER8.[68]

Molecular dynamics simulations were run using the sander module of AMBER8 and the parm98 parameters for the protein. The charge distribution of the inhibitor was determined from a fit to the HF/6s-31G(d) electrostatic potential obtained with Gaussian'03[69] using the RESP procedure,[70] and the van der Waals parameters were taken from those defined for related atoms in the AMBER force field. The system was partitioned into a mobile region, which included the ligand, all the protein residues containing at least one atom within 20 Å from the ligand, and all the water molecules and Na^+ cations. The geometry of the system was minimized in four steps. First, the position of hydrogen atoms was optimized using 3000 steps of steepest descent algorithm. Then water molecules were refined through 2000 steps of steepest descent followed by 3000 steps of conjugate gradient. Next, the ligand, water molecules, and counterions were optimized with 2000 steps of steepest descent and 4000 steps of conjugate gradient, and finally the whole system was optimized with 3000 steps of steepest descent and 7000 steps of conjugate gradient. Thermalization of the mobile part of the system was performed in five steps of 20 ps, incrementing the temperature up to 298 K. At this point, a 10 ns molecular dynamics simulation was carried out using a time step of 1 fs. SHAKE was used for those bonds containing hydrogen atoms, and a cutoff of 11 Å was used for nonbonded interactions.

The analysis of the structural features that mediate the binding mode to the enzyme was determined by averaging the parameters for the snapshots (saved every picosecond) sampled along the last 5 ns of the molecular dynamics simulations.

Acknowledgment. Financial support from Dirección General de Investigación of Ministerio de Ciencia y Tecnología and FEDER (Projects CTQ2005-02192/BQU, SAF2006-04339, CTQ2005-09365, and SAF2005-01604) and Comissionat per a

Universitats i Recerca of the Generalitat de Catalunya (Projects 2005-SGR00180, 2001-SGR00216, and 2005-SGR00893) are gratefully acknowledged. We also thank the Serveis Científico-Tècnics of the University of Barcelona for NMR facilities, and we thank P. Domènech from the IIQAB (CSIC, Barcelona, Spain) for carrying out the elemental analyses.

Supporting Information Available: Experimental procedures, spectral and analytical characterization data of all of the new compounds (except for **8a**, **10a**, and **14a**) and the known compounds **13** and **19**, and the predicted pose of donepezil obtained by using GOLD. This material is available free of charge via the Internet at http://pubs.acs.org.

References

(1) Pang, Y.-P.; Quiram, P.; Jelacic, T.; Hong, F.; Brimijoin, S. Highly Potent, Selective, and Low Cost Bis-tetrahydroaminacrine Inhibitors of Acetylcholinesterase. *J. Biol. Chem.* **1996**, *271*, 23646–23649.

(2) Du, D.-M.; Carlier, P. R. Development of Bivalent Acetylcholinesterase Inhibitors as Potential Therapeutic Drugs for Alzheimer's Disease. *Curr. Pharm. Des.* **2004**, *10*, 3141–3156.

(3) Li, W. M.; Kan, K. K. W.; Carlier, P. R.; Pang, Y. P.; Han, Y. F. Easts Meets West in the Search for Alzheimer's Therapeutics. Novel Dimeric Inhibitors from Tacrine and Huperzine A. *Curr. Alzheimer Res.* **2007**, *4*, 386–396.

(4) Recanatini, M.; Valenti, P. Acetylcholinesterase Inhibitors as a Starting Point towards Improved Alzheimer's Disease Therapeutics. *Curr. Pharm. Des.* **2004**, *10*, 3157–3166.

(5) Muñoz-Torrero, D.; Camps, P. Dimeric and Hybrid Anti-Alzheimer Drug Candidates. *Curr. Med. Chem.* **2006**, *13*, 763–771.

(6) Castro, A.; Martinez, A. Targeting Beta-Amyloid Pathogenesis through Acetylcholinesterase Inhibitors. *Curr. Pharm. Des.* **2006**, *12*, 4377–4387.

(7) Holzgrabe, U.; Kapková, P.; Alptüzün, V.; Scheiber, J.; Kugelmann, E. Targeting Acetylcholinesterase To Treat Neurodegeneration. *Expert Opin. Ther. Targets* **2007**, *11*, 161–179.

(8) Cavalli, A.; Bolognesi, M. L.; Minarini, A.; Rosini, M.; Tumiatti, V.; Recanatini, M.; Melchiorre, C. Multi-Target-Directed Ligands To Combat Neurodegenerative Diseases. *J. Med. Chem.* **2008**, *51*, 347–372.

(9) Piazzi, L.; Rampa, A.; Bisi, A.; Gobbi, S.; Belluti, F.; Cavalli, A.; Bartolini, M.; Andrisano, V.; Valenti, P.; Recanatini, M. 3-(4-{[Benzyl(methyl)amino]methyl}phenyl)-6,7-dimethoxy-2*H*-2-chromenone (AP2238) Inhibits Both Acetylcholinesterase and Acetylcholinesterase-Induced β-Amyloid Aggregation: A Dual Function Lead for Alzheimer's Disease Therapy. *J. Med. Chem.* **2003**, *46*, 2279–2282.

(10) Bolognesi, M. L.; Andrisano, V.; Bartolini, M.; Banzi, R.; Melchiorre, C. Propidium-Based Polyamine Ligands as Potent Inhibitors of Acetylcholinesterase and Acetylcholinesterase-Induced Amyloid-β Aggregation. *J. Med. Chem.* **2005**, *48*, 24–27.

(11) Rosini, M.; Andrisano, V.; Bartolini, M.; Bolognesi, M. L.; Hrelia, P.; Minarini, A.; Tarozzi, A.; Melchiorre, C. Rational Approach To Discover Multipotent Anti-Alzheimer Drugs. *J. Med. Chem.* **2005**, *48*, 360–363.

(12) Muñoz-Ruiz, P.; Rubio, L.; García-Palomero, E.; Dorronsoro, I.; del Monte-Millán, M.; Valenzuela, R.; Usán, P.; de Austria, C.; Bartolini, M.; Andrisano, V.; Bidon-Chanal, A.; Orozco, M.; Luque, F. J.; Medina, M.; Martínez, A. Design, Synthesis, and Biological Evaluation of Dual Binding Site Acetylcholinesterase Inhibitors: New Disease-Modifying Agents for Alzheimer's Disease. *J. Med. Chem.* **2005**, *48*, 7223–7233.

(13) Belluti, F.; Rampa, A.; Piazzi, L.; Bisi, A.; Gobbi, S.; Bartolini, M.; Andrisano, V.; Cavalli, A.; Recanatini, M.; Valenti, P. Cholinesterase Inhibitors: Xanthostigmine Derivatives Blocking the Acetylcholinesterase-Induced β-Amyloid Aggregation. *J. Med. Chem.* **2005**, *48*, 4444–4456.

(14) Piazzi, L.; Cavalli, A.; Belluti, F.; Bisi, A.; Gobbi, S.; Rizzo, S.; Bartolini, M.; Andrisano, V.; Recanatini, M.; Rampa, A. Extensive SAR and Computational Studies of 3-{4-[(Benzylmethylamino)methyl]phenyl}-6,7-dimethoxy-2*H*-2-chromenone (AP2238) Derivatives. *J. Med. Chem.* **2007**, *50*, 4250–4254.

(15) Cavalli, A.; Bolognesi, M. L.; Capsoni, S.; Andrisano, V.; Bartolini, M.; Margotti, E.; Cattaneo, A.; Recanatini, M.; Melchiorre, C. A Small Molecule Targeting the Multifactorial Nature of Alzheimer's Disease. *Angew. Chem., Int. Ed.* **2007**, *46*, 3689–3692.

(16) Bolognesi, M. L.; Banzi, R.; Bartolini, M.; Cavalli, A.; Tarozzi, A.; Andrisano, V.; Minarini, A.; Rosini, M.; Tumiatti, V.; Bergamini, C.; Fato, R.; Lenaz, G.; Hrelia, P.; Cattaneo, A.; Recanatini, M.; Melchiorre, C. Novel Class of Quinone-Bearing Polyamines as Multi-Target-Directed Ligands To Combat Alzheimer's Disease. *J. Med. Chem.* **2007**, *50*, 4882–4897.

(17) Bolognesi, M. L.; Cavalli, A.; Valgimigli, L.; Bartolini, M.; Rosini, M.; Andrisano, V.; Recanatini, M.; Melchiorre, C. Multi-Target-Directed Drug Design Strategy: From a Dual Binding Site Acetylcholinesterase Inhibitor to a Trifunctional Compound against Alzheimer's Disease. *J. Med. Chem.* **2007**, *50*, 6446–6449.

(18) Kwon, Y. E.; Park, J. Y.; No, K. T.; Shin, J. H.; Lee, S. K.; Eun, J. S.; Yang, J. H.; Shin, T. Y.; Kim, D. K.; Chae, B. S.; Leem, J.-Y.; Kim, K. H. Synthesis, in Vitro Assay, and Molecular Modeling of New Piperidine Derivatives Having Dual Inhibitory Potency against Acetylcholinesterase and $A\beta_{1-42}$ Aggregation for Alzheimer's Disease Therapeutics. *Bioorg. Med. Chem.* **2007**, *15*, 6596–6607.

(19) Skovronsky, D. M.; Lee, V. M.-Y.; Trojanowski, J. Q. Neurodegenerative Diseases: New Concepts of Pathogenesis and Their Therapeutic Implications. *Annu. Rev. Pathol. Mech. Dis.* **2006**, *1*, 151–170.

(20) De Ferrari, G. V.; Canales, M. A.; Shin, I.; Weiner, L. M.; Silman, I.; Inestrosa, N. C. A Structural Motif of Acetylcholinesterase That Promotes Amyloid Beta-Peptide Fibril Formation. *Biochemistry* **2001**, *40*, 10447–10457.

(21) Sugimoto, H.; Iimura, Y.; Yamanishi, Y.; Yamatsu, K. Synthesis and Structure−Activity Relationships of Acetylcholinesterase Inhibitors: 1-Benzyl-4-[(5,6-dimethoxy-1-oxoindan-2-yl)methyl]piperidine Hydrochloride and Related Compounds. *J. Med. Chem.* **1995**, *38*, 4821–4829.

(22) Kryger, G.; Silman, I.; Sussman, J. L. Structure of Acetylcholinesterase Complexed with E2020 (Aricept): Implications for the Design of New Anti-Alzheimer Drugs. *Structure* **1999**, *7*, 297–307.

(23) Bartolini, M.; Bertucci, C.; Cavrini, V.; Andrisano, V. β-Amyloid Aggregation Induced by Human Acetylcholinesterase: Inhibition Studies. *Biochem. Pharmacol.* **2003**, *65*, 407–416.

(24) Carlier, P. R.; Du, D. -M.; Han, Y.; Liu, J.; Pang, Y.-P. Potent, Easily Synthesized Huperzine A-Tacrine Hybrid Acetylcholinesterase Inhibitors. *Bioorg. Med. Chem. Lett.* **1999**, *9*, 2335–2338.

(25) Savini, L.; Campiani, G.; Gaeta, A.; Pellerano, C.; Fattorusso, C.; Chiasserini, L.; Fedorko, J. M.; Saxena, A. Novel and Potent Tacrine-Related Hetero- and Homobivalent Ligands for Acetylcholinesterase and Butyrylcholinesterase. *Bioorg. Med. Chem. Lett.* **2001**, *11*, 1779–1782.

(26) Hu, M.-K.; Wu, L.-J.; Hsiao, G.; Yen, M.-H. Homodimeric Tacrine Congeners as Acetylcholinesterase Inhibitors. *J. Med. Chem.* **2002**, *45*, 2277–2282.

(27) Lewis, W. G.; Green, L. G.; Grynszpan, F.; Radić, Z.; Carlier, P. R.; Taylor, P.; Finn, M. G.; Sharpless, K. B. Click Chemistry in Situ: Acetylcholinesterase as a Reaction Vessel for the Selective Assembly of a Femtomolar Inhibitor from an Array of Building Blocks. *Angew. Chem., Int. Ed.* **2002**, *41*, 1053–1057.

(28) Savini, L.; Gaeta, A.; Fattorusso, C.; Catalanotti, B.; Campiani, G.; Chiasserini, L.; Pellerano, C.; Novellino, E.; McKissic, D.; Saxena, A. Specific Targeting of Acetylcholinesterase and Butyrylcholinesterase Recognition Sites. Rational Design of Novel, Selective, and Highly Potent Cholinesterase Inhibitors. *J. Med. Chem.* **2003**, *46*, 1–4.

(29) Camps, P.; Formosa, X.; Muñoz-Torrero, D.; Petrignet, J.; Badia, A.; Clos, M. V. Synthesis and Pharmacological Evaluation of Huprine−Tacrine Heterodimers: Subnanomolar Dual Binding Site Acetylcholinesterase Inhibitors. *J. Med. Chem.* **2005**, *48*, 1701–1704.

(30) Shao, D.; Zou, C.; Luo, C.; Tang, X.; Li, Y. Synthesis and Evaluation of Tacrine-E2020 Hybrids as Acetylcholinesterase Inhibitors for the Treatment of Alzheimer's Disease. *Bioorg. Med. Chem. Lett.* **2004**, *14*, 4639–4642.

(31) Alonso, D.; Dorronsoro, I.; Rubio, L.; Muñoz, P.; García-Palomero, E.; Del Monte, M.; Bidon-Chanal, A.; Orozco, M.; Luque, F. J.; Castro, A.; Medina, M.; Martínez, A. Donepezil−Tacrine Hybrid Related Derivatives as New Dual Binding Site Inhibitors of AChE. *Bioorg. Med. Chem.* **2005**, *13*, 6588–6597.

(32) Gemma, S.; Gabellieri, E.; Huleatt, P.; Fatorusso, C.; Borriello, M.; Catalanotti, B.; Butini, S.; De Angelis, M.; Novellino, E.; Nacci, V.; Belinskaya, T.; Saxena, A.; Campiani, G. Discovery of Huperzine A-Tacrine Hybrids as Potent Inhibitors of Human Cholinesterases Targeting Their Midgorge Recognition Sites. *J. Med. Chem.* **2006**, *49*, 3421–3425.

(33) Elsinghorst, P. W.; González Tanarro, C. M.; Gütschow, M. Novel Heterobivalent Tacrine Derivatives as Cholinesterase Inhibitors with Notable Selectivity Toward Butyrylcholinesterase. *J. Med. Chem.* **2006**, *49*, 7540–7544.

(34) Elsinghorst, P. W.; Cieslik, J. S.; Mohr, K.; Tränkle, C.; Gütschow, M. First Gallamine−Tacrine Hybrid: Design and Characterization at Cholinesterases and the M_2 Muscarinic Receptor. *J. Med. Chem.* **2007**, *50*, 5685–5695.

(35) Harel, M.; Schalk, I.; Ehret-Sabatier, L.; Bouet, F.; Goeldner, M.; Hirth, C.; Axelsen, P.; Silman, I.; Sussman, J. L. Quaternary Ligand Binding to Aromatic Residues in the Active-Site Gorge of Acetylcholinesterase. *Proc. Natl. Acad. Sci. U.S.A.* **1993**, *90*, 9031–9035.
(36) Wlodek, S. T.; Antosiewicz, J.; McCammon, J. A.; Straatsma, T. P.; Gilson, M. K.; Briggs, J. M.; Humblet, C.; Sussman, J. L. Binding of Tacrine and 6-Chlorotacrine by Acetylcholinesterase. *Biopolymers* **1996**, *38*, 109–117.
(37) Recanatini, M.; Cavalli, A.; Belluti, F.; Piazzi, L.; Rampa, A.; Bisi, A.; Gobbi, S.; Valenti, P.; Andrisano, V.; Bartolini, M.; Cavrini, V. SAR of 9-Amino-1,2,3,4-tetrahydroacridine-Based Acetylcholinesterase Inhibitors: Synthesis, Enzyme Inhibitory Activity, QSAR, and Structure-Based CoMFA of Tacrine Analogues. *J. Med. Chem.* **2000**, *43*, 2007–2018.
(38) Dvir, H.; Wong, D. M.; Harel, M.; Barril, X.; Orozco, M.; Luque, F. J.; Muñoz-Torrero, D.; Camps, P.; Rosenberry, T. L.; Silman, I.; Sussman, J. L. 3D Structure of *Torpedo californica* Acetylcholinesterase Complexed with Huprine X at 2.1 Å Resolution: Kinetic and Molecular Dynamic Correlates. *Biochemistry* **2002**, *41*, 2970–2981.
(39) Hu, M.-K.; Lu, C.-F. A Facile Synthesis of Bis-Tacrine Isosteres. *Tetrahedron Lett.* **2000**, *41*, 1815–1818.
(40) Michalson, E. T.; D'Andrea, S.; Freeman, J. P.; Szmuszkovicz, J. The Synthesis of 9-(1-Azetidinyl)-1,2,3,4-tetrahydroacridine. *Heterocycles* **1990**, *30*, 415–425.
(41) Elati, C. R.; Kolla, N.; Chalamala, S. R.; Vankawala, P. J.; Sundaram, V.; Vurimidi, H.; Mathad, V. T. New Synthesis of Donepezil through Palladium-Catalyzed Hydrogenation Approach. *Synth. Commun.* **2006**, *36*, 169–174.
(42) Lee, S.-Y.; Choe, Y. S.; Sugimoto, H.; Kim, S. E.; Hwang, S. H.; Lee, K.-H.; Choi, Y.; Lee, J.; Kim, B.-T. Synthesis and Biological Evaluation of 1-(4-[^{18}F]Fluorobenzyl-4-[5,6-dimethoxy-1-oxoindan-2-yl)methyl]piperidine for in Vivo Studies of Acetylcholinesterase. *Nuclear Med. Biol.* **2000**, *27*, 741–744.
(43) Inoue, A.; Kawai, T.; Wakita, M.; Iimura, Y.; Sugimoto, H.; Kawakami, Y. The Simulated Binding of (±)-2,3-Dihydro-5,6-dimethoxy-2-[[1-(phenylmethyl)-4-piperidinyl]methyl]-1*H*-inden-1-one Hydrochloride (E2020) and Related Inhibitors to Free and Acylated Acetylcholinesterases and Corresponding Structure−Activity Analyses. *J. Med. Chem.* **1996**, *39*, 4460–4470.
(44) Reddy, K. V. S. R. K.; Babu, J. M.; Kumar, P. A.; Chandrashekar, E. R. R.; Mathad, V. T.; Eswaraiah, S.; Reddy, M. S.; Vyas, K. Identification and Characterization of Potential Impurities of Donepezil. *J. Pharm. Biomed. Anal.* **2004**, *35*, 1047–1058.
(45) Galanakis, D.; Davis, C. A.; Ganellin, C. R.; Dunn, P. M. Synthesis and Quantitative Structure−Activity Relationship of a Novel Series of Small Conductance Ca^{2+}-Activated K^+ Channel Blockers Related to Dequalinium. *J. Med. Chem.* **1996**, *39*, 359–370.
(46) Carlier, P. R.; Chow, E. S.-H.; Han, Y.; Liu, J.; El Yazal, J.; Pang, Y.-P. Heterodimeric Tacrine-Based Acetylcholinesterase Inhibitors: Investigating Ligand-Peripheral Site Interactions. *J. Med. Chem.* **1999**, *42*, 4225–4231.
(47) Ellman, G. L.; Courtney, K. D.; Andres, B., Jr.; Featherstone, R. M. A New and Rapid Colorimetric Determination of Acetylcholinesterase Activity. *Biochem. Pharmacol.* **1961**, *7*, 88–95.
(48) Giacobini, E. Cholinesterase Inhibitors: New Roles and Therapeutic Alternatives. *Pharmacol. Res.* **2004**, *50*, 433–440.
(49) Lane, R. M.; Potkin, S. G.; Enz, A. Targeting Acetylcholinesterase and Butyrylcholinesterase in Dementia. *Int. J. Neuropsychopharmacol.* **2005**, *9*, 1–24.
(50) Inestrosa, N. C.; Alvarez, A.; Pérez, C. A.; Moreno, R. D.; Vicente, M.; Linker, C.; Casanueva, O. I.; Soto, C.; Garrido, J. Acetylcholinesterase Accelerates Assembly of Amyloid-β-Peptides into Alzheimer's Fibrils: Possible Role of the Peripheral Site of the Enzyme. *Neuron* **1996**, *16*, 881–891.
(51) Alvarez, A.; Alarcón, R.; Opazo, C.; Campos, E. O.; Muñoz, F. J.; Calderón, F. H.; Dajas, F.; Gentry, M. K.; Doctor, B. P.; De Mello, F. G.; Inestrosa, N. C. Stable Complexes Involving Acetylcholinesterase and Amyloid-β-Peptide Change the Biochemical Properties of the Enzyme and Increase the Neurotoxicity of Alzheimer's Fibrils. *J. Neurosci.* **1998**, *18*, 3213–3223.
(52) Taylor, P.; Lappi, S. Interaction of Fluorescence Probes with Acetylcholinesterase. The Site and Specificity of Propidium Binding. *Biochemistry* **1975**, *14*, 1989–1997.
(53) Camps, P.; Cusack, B.; Mallender, W. D.; El Achab, R.; Morral, J.; Muñoz-Torrero, D.; Rosenberry, T. L. Huprine X Is a Novel High-Affinity Inhibitor of Acetylcholinesterase That Is of Interest for Treatment of Alzheimer's Disease. *Mol. Pharmacol.* **2000**, *57*, 409–417.
(54) LeVine, H., III. Quantification of β-Sheet Amyloid Fibril Structures with Thioflavin T. *Methods Enzymol.* **1999**, *309*, 274–284.
(55) Eisert, R.; Felau, L.; Brown, L. R. Methods for Enhancing the Accuracy and Reproducibility of Congo Red and Thioflavin T Assays. *Anal. Biochem.* **2006**, *353*, 144–146.
(56) De Ferrari, G. V.; Mallender, W. D.; Inestrosa, N. C.; Rosenberry, T. L. Thioflavin T Is a Fluorescent Probe of the Acetylcholinesterase Peripheral Site That Reveals Conformational Interactions between the Peripheral and Acylation Sites. *J. Biol. Chem.* **2001**, *276*, 23282–23287.
(57) Vericat, J. A.; Muñoz, P.; Windisch, M.; Hutter-Paier, B.; Medina, M.; Martinez, A. Presented at the 5th Neurobiology of Aging Conference, San Diego, CA, 2004.
(58) http://www.neuropharma.es.
(59) Camps, P.; El Achab, R.; Morral, J.; Muñoz-Torrero, D.; Badia, A.; Baños, J. E.; Vivas, N. M.; Barril, X.; Orozco, M.; Luque, F. J. New Tacrine−Huperzine A Hybrids (Huprines): Highly Potent Tight-Binding Acetylcholinesterase Inhibitors of Interest for the Treatment of Alzheimer's Disease. *J. Med. Chem.* **2000**, *43*, 4657–4666.
(60) Senapati, S.; Bui, J. M.; McCammon, J. A. Induced Fit in Mouse Acetylcholinesterase upon Binding a Femtomolar Inhibitor: A Molecular Dynamics Study. *J. Med. Chem.* **2005**, *48*, 8155–8162.
(61) Bourne, Y.; Radic, Z.; Kolb, H. C.; Sharpless, K. B.; Taylor, P.; Marchot, P. Structural Insights into Conformational Flexibility at the Peripheral Site and within the Active Center Gorge of AChE. *Chem.-Biol. Interact.* **2005**, *157−158*, 159–165.
(62) Colletier, J. Ph.; Sanson, B.; Nachon, F.; Gabellieri, E.; Fattorusso, C.; Campiani, G.; Weik, M. Conformational Flexibility in the Peripheral Site of *Torpedo californica* Acetylcholinesterase Revealed by the Complex Structure with a Bifunctional Inhibitor. *J. Am. Chem. Soc.* **2006**, *128*, 4526–4527.
(63) Aguado, F.; Badía, A.; Baños, J. E.; Bosch, F.; Bozzo, C.; Camps, P.; Contreras, J.; Dierssen, M.; Escolano, C.; Görbig, D. M.; Muñoz-Torrero, D.; Pujol, M. D.; Simón, M.; Vázquez, M. T.; Vivas, N. M. Synthesis and Evaluation of Tacrine-Related Compounds for the Treatment of Alzheimer's Disease. *Eur. J. Med. Chem.* **1994**, *29*, 205–221.
(64) Kryger, G.; Harel, M.; Giles, K.; Toker, L.; Velan, B.; Lazar, A.; Kronman, C.; Barak, D.; Ariel, N.; Shafferman, A.; Silman, I.; Sussman, J. L. Structures of Recombinant Native and E202Q Mutant Human Acetylcholinesterase Complexed with the Snake-Venom Toxin Fasciculin-II. *Acta Cystallogr., Sect. D: Biol. Crystallogr.* **2000**, *56*, 1385–1394.
(65) *InsightII*; Accelrys Inc.: San Diego, CA, 1996.
(66) Jones, G.; Willet, P.; Glen, R. C.; Leach, A. R.; Taylor, R. Development and Validation of a Genetic Algorithm for Flexible Docking. *J. Mol. Biol.* **1997**, *267*, 727–748.
(67) Jorgensen, W. L.; Chandrasekhar, J.; Madura, J. D.; Impey, R. W.; Klein, M. L. Comparison of Simple Potential Functions for Simulating Liquid Water. *J. Chem. Phys.* **1983**, *79*, 926–935.
(68) Case, D. A.; Darden, T. A.; Cheatham, T. E.; Pearlman, D. A.; Simmerling, C. L.; Wang, J.; Duke, R. E.; Luo, R.; Merz, K. M.; Pearlman, D. A.; Crowley, M. ; Brozell, S.; Tsui, V.; Gohlke, H.; Mongan, J.; Hornak, V.; Cui, G.; Beroza, P.; Schafmeister, P.; Caldwell, J. W.; Ross, W. S.; Kollman, P. A. *AMBER8*; University of California: San Francisco, CA, 2004.
(69) Frisch, M. J.; Trucks, G. W.; Schlegel, H. B.; Scuseria, G. E.; Robb, M. A.; Cheeseman, J. R.; Montgomery, J. A., Jr.; Vreven, T.; Kudin, K. N.; Burant, J. C.; Millam, J. M.; Iyengar, S. S.; Tomasi, J.; Barone, V.; Mennucci, B.; Cossi, M.; Scalmani, G.; Rega, N.; Petersson, G. A.; Nakatsuji, H.; Hada, M.; Ehara, M.; Toyota, K.; Fukuda, R.; Hasegawa, J.; Ishida, M.; Nakajima, T.; Honda, Y.; Kitao, O.; Nakai, H.; Klene, M.; Li, X.; Knox, J. E.; Hratchian, H. P.; Cross, J. B.; Adamo, C.; Jaramillo, J.; Gomperts, R.; Stratmann, R. E.; Yazyev, O.; Austin, A. J.; Cammi, R.; Pomelli, C.; Ochterski, J. W.; Ayala, P. Y.; Morokuma, K.; Voth, G. A.; Salvador, P.; Dannenberg, J. J.; Zakrzewski, V. G.; Dapprich, S.; Daniels, A. D.; Strain, M. C.; Farkas, O.; Malick, D. K.; Rabuck, A. D.; Raghavachari, K.; Foresman, J. B.; Ortiz, J. V.; Cui, Q.; Baboul, A. G.; Clifford, S.; Cioslowski, J.; Stefanov, B. B.; Liu, G.; Liashenko, A.; Piskorz, P.; Komaromi, I.; Martin, R. L.; Fox, D. J.; Keith, T.; Al-Laham, M. A.; Peng, C. Y.; Nanayakkara, A.; Challacombe, M.; Gill, P. M. W.; Johnson, B.; Chen, W.; Wong, M. W.; Gonzalez, C.; Pople, J. A. *Gaussian 03*, revision B.04; Gaussian, Inc.: Pittsburgh, PA, 2003.
(70) Bayly, C. I.; Cieplak, P.; Cornell, W. D.; Kollman, P. A. A Well-Behaved Electrostatic Potential Based Method Using Charge Restraints for Deriving Atomic Charges. *J. Phys. Chem.* **1993**, *97*, 10269–10280.

JM8001313